

Testing of planar hydrogenated amorphous silicon sensors with charge selective contacts for the construction of 3D- detectors.

M. Menichelli^{1,*}, M. Bizzarri^{1,2}, M. Boscardin^{3,4}, M. Caprai¹, A.P. Caricato⁵, G.A.P. Cirrone⁶, M. Crivellari⁴, I. Cupparo⁷, G. Cuttone⁶, S. Dunand⁸, L. Fanò^{1,2}, O. Hammad⁴, M. Ionica¹, K. Kanxheri¹, M. Large¹⁰, G. Maruccio⁵, A.G. Monteduro⁵, A. Morozzi¹, F. Moscatelli^{1,9}, A. Papi¹, D. Passeri^{1,11}, M. Petasecca¹⁰, G. Petringa⁶, G. Quarta⁵, S. Rizzato⁵, A. Rossi^{1,2}, G. Rossi¹, A. Scorzoni^{1,11}, L. Servoli¹, C. Talamonti⁷, G. Verzellesi^{3,12}, N. Wyrsh⁸.

¹. INFN, Sez. di Perugia, via Pascoli s.n.c. 06123 Perugia (ITALY)

². Dip. di Fisica e Geologia dell'Università degli Studi di Perugia, via Pascoli s.n.c. 06123 Perugia (ITALY)

³. INFN, TIPFA Via Sommarive 14, 38123 Povo (TN) (ITALY)

⁴. Fondazione Bruno Kessler, Via Sommarive 18, 38123 Povo (TN) (ITALY)

⁵. INFN and Department of Mathematics and Physics "Ennio de Giorgi" University of Salento, Via per Arnesano, 73100 Lecce (ITALY)

⁶. INFN Laboratori Nazionali del Sud, Via S. Sofia 62, 95123 Catania (ITALY)

⁷. INFN and Dipartimento di Fisica Scienze Biomediche sperimentali e Cliniche "Mario Serio", Viale Morgagni 50, 50135 Firenze (FI) (ITALY)

⁸. Ecole Polytechnique Fédérale de Lausanne (EPFL), Photovoltaic and Thin-Film Electronics Laboratory (PV-Lab), Rue de la Maladière 71b, 2000 Neuchâtel, (SWITZERLAND).

⁹. CNR-IOM, via Pascoli s.n.c. 06123 Perugia (ITALY)

¹⁰. Centre for Medical Radiation Physics, University of Wollongong, Northfields Ave Wollongong NSW 2522, (AUSTRALIA).

¹¹. Dip. di Ingegneria dell'Università degli studi di Perugia, via G. Duranti 06125 Perugia (ITALY)

¹². Dip. di Scienze e Metodi dell'Ingegneria, Università di Modena e Reggio Emilia, Via Amendola 2, 42122 Reggio Emilia (ITALY)

* Corresponding author, Mauro.menichelli@pg.infn.it

Abstract

Hydrogenated Amorphous Silicon (a-Si:H) is a material well known for its intrinsic radiation hardness and is primarily utilized in solar cells as well as for particle detection and dosimetry. Planar p-i-n diode detectors are fabricated entirely by means of intrinsic and doped PECVD of a mixture of Silane (SiH₄) and molecular Hydrogen. In order to develop 3D detector geometries using a-Si:H, two options for the junction fabrication have been considered: ion implantation and charge selective contacts through atomic layer deposition. In order to test the functionality of the charge selective contact electrodes, planar detectors have been fabricated utilizing this technique. In this paper, we provide a general overview of the 3D fabrication project followed by the results of leakage current measurements and x-ray dosimetric tests performed on planar diodes containing charge selective contacts to investigate the feasibility of the charge selective contact methodology for integration with the proposed 3D detector architectures.

1. Introduction

Hydrogenated amorphous silicon (a-Si:H) has remarkable radiation resistance properties and can be deposited on a variety of different substrates. The motivations for the construction of a 3D a-Si:H detector are described in ref. [1]. During 3D detector fabrication, once the a-Si:H substrate is grown, holes (or trenches) should be made in the substrate in order to prepare cavities for electrode manufacturing. Once the holes are etched their walls should then be doped in order to build the basic p-i-n electrode structure of the detector. Since commonly used techniques for planar structures (i.e. PECVD deposition of doped a-Si:H) are unable to achieve a conformal coating of the walls of the etched holes, two alternative options will be considered. The first option is the Atomic Layer Deposition (ALD) of conductive metallic oxides for the creation of selective contacts for each type of charge carrier. Titanium or aluminum doped zinc oxide (AZO) will be used as an electron selective contact and molybdenum oxide will be used for hole collection. This technique has been adopted in the construction of solar cells and, for the first time, is documented here in its use for detector fabrication. This charge collection mechanism is based on the different mobilities of holes and electrons within the two sets of selective contact materials previously identified. These selective contact materials aim to utilize the fact that the mobility should be large for electrons and small for holes in the electron selective contact and the opposite in the hole selective contact [2]. The second option is the Ion implantation of Phosphor ions for n-type doping and Boron for p-type doping.

In this paper we will describe the testing of planar diodes utilizing charge selective contacts to assess their performance as radiation detectors. Specifically, the leakage current versus bias voltage for various samples and configurations (different thicknesses and charge selective contact materials) and the linearity of response to different x-ray dose rates will be measured. From this, the charge sensitivity will be extracted both at 0V and under an applied bias for the tested devices.

2. Description of the samples and leakage current measurements

In order to assess the performance of the charge selective contact devices for particle detection and dosimetry two sets of devices deposited on glass have been fabricated according to the scheme shown in figure 1a, while figure 1b shows a picture of the detector seen from above.

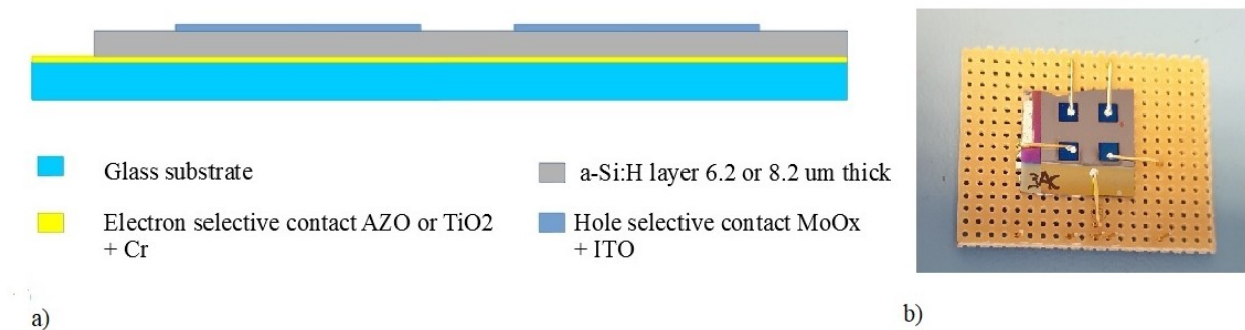


Fig.1 a) Layout of the detector (lateral view) b) Picture of the detector seen from above.

The detector architecture consists of electron selective contacts in the form of ZnO:Al (AZO) or TiO₂ layers deposited on glass, with thicknesses of 60 nm or 10 nm, respectively. The active detector layer is made of a-Si:H in two different thickness: 6.2 and 8.2 microns. Hole selective contacts were made of 20 nm thick MoO_x protected by a 60 nm thick indium tin oxide (ITO) layer. These hole

selective contacts were deposited via sputtering resulting in four square electrodes having a $5 \times 5 \text{ mm}^2$ area. For initial leakage current measurements, the detectors were biased using a Keithley 2410-C SMU to an electric field of up to $5 \text{ V}/\mu\text{m}$. Fig. 2 displays the resulting leakage currents versus bias voltage for the tested devices.

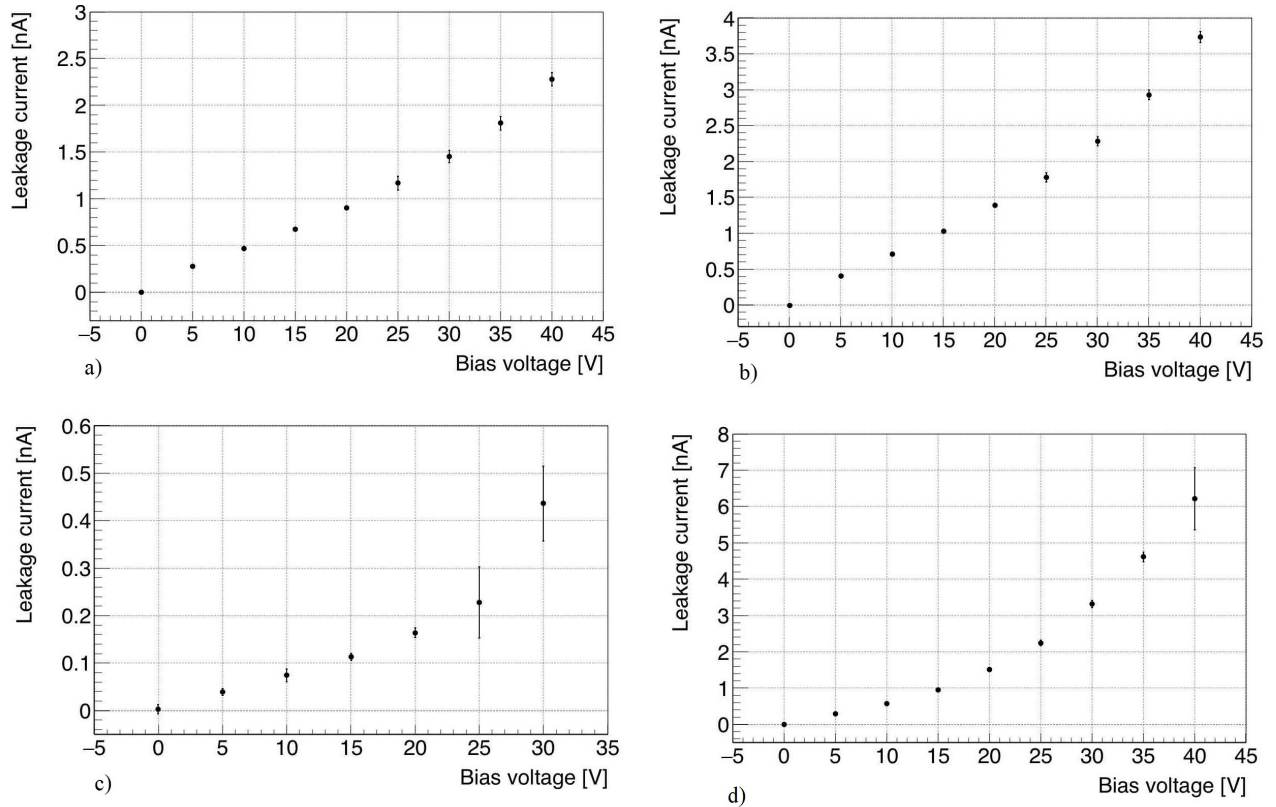


Fig. 2 Leakage current measurements of various devices in a-Si:H layer having different thicknesses and electron selective contact materials. a) AZO electron selective contacts with a-Si:H layer having $8.2 \mu\text{m}$ thickness (Sample 1). b) AZO electron selective contacts with a-Si:H layer having $8.2 \mu\text{m}$ thickness (Sample 2). c) AZO electron selective contacts with a-Si:H layer having $6.2 \mu\text{m}$ thickness. d) Titanium Oxide electron selective contacts with a-Si:H layer having $8.2 \mu\text{m}$ thickness.

From the data presented in Fig. 2 it is observed that AZO devices have a lower leakage current compared to TiO_2 devices, and that thinner devices at the same field have a lower current in comparison to their thicker counterparts in agreement with what reported in for doped contacts ref. [3]. The overall value of the leakage current normalized to surface for an $8.2 \mu\text{m}$ device with AZO selective contact at $5 \text{ V}/\mu\text{m}$ bias is in the order of $9.2 \text{ nA}/\text{cm}^2$ for sample 1 and $14.8 \text{ nA}/\text{cm}^2$ for sample 2, while for the TiO_2 device is $24.4 \text{ nA}/\text{cm}^2$. For the AZO device having thickness $6.2 \mu\text{m}$ the leakage current per unit area under the same $5 \text{ V}/\mu\text{m}$ biasing field is $1.76 \text{ nA}/\text{cm}^2$. Results are summarized in Table 1.

Description of sample	Current density @ 30 V (nA/cm ²)	Current density @ 40 V
8.2 μm AZO electron selective contact. Sample 1	5.8	9.2
8.2 μm AZO electron selective contact. Sample 2	9.2	14.8
6.2 μm AZO electron selective contact.	1.76	N/A
8.2 μm TiO ₂ electron selective contact.	12.8	24.4

Table 1. Current density for the 4 samples at 30 V and 40 V bias.

3. Current versus X-ray doses response in charge selective contact devices.

For preliminary determinations of the performance of the charge selective contact devices for dosimetry, the devices were irradiated using a miniature X-ray tube from Newton Scientific [4] having 50 kV maximum voltage, 200 μA maximum current (10 W maximum power), and a 125 μm Be window. The irradiation setup is shown in Fig. 3.

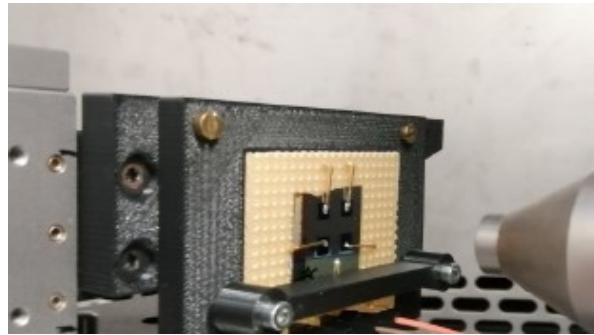


Fig.3 Irradiation test setup.

The X-ray tube was configured to deliver dose rates in the range of 0-22 mGy/s, with the response of the device calculated as the induced current to a beam exposure minus leakage current (at 0 Gy dose). For each of the device architectures investigated two measurements were performed: a first set of measurements with devices at 0V bias (photovoltaic mode) and a second set of measurements with devices under a non-zero applied bias (30 V for samples with 8.2 μm active layer thickness and 20V for the 6.2 μm thick sample). The results of measurements conducted at 0V bias are indicative of the devices performance for personal dosimetry in clinical applications, whilst their operation under a non-zero bias allows for the enhancement of the device sensitivities to assess their operation in the framework of the proposed 3D detector geometries as well as for beam monitoring applications. The test is performed by changing the tube current and measuring the device under test (DUT) current. Before the measurement a calibration of dose rate versus tube current in the same position of the detector is performed.

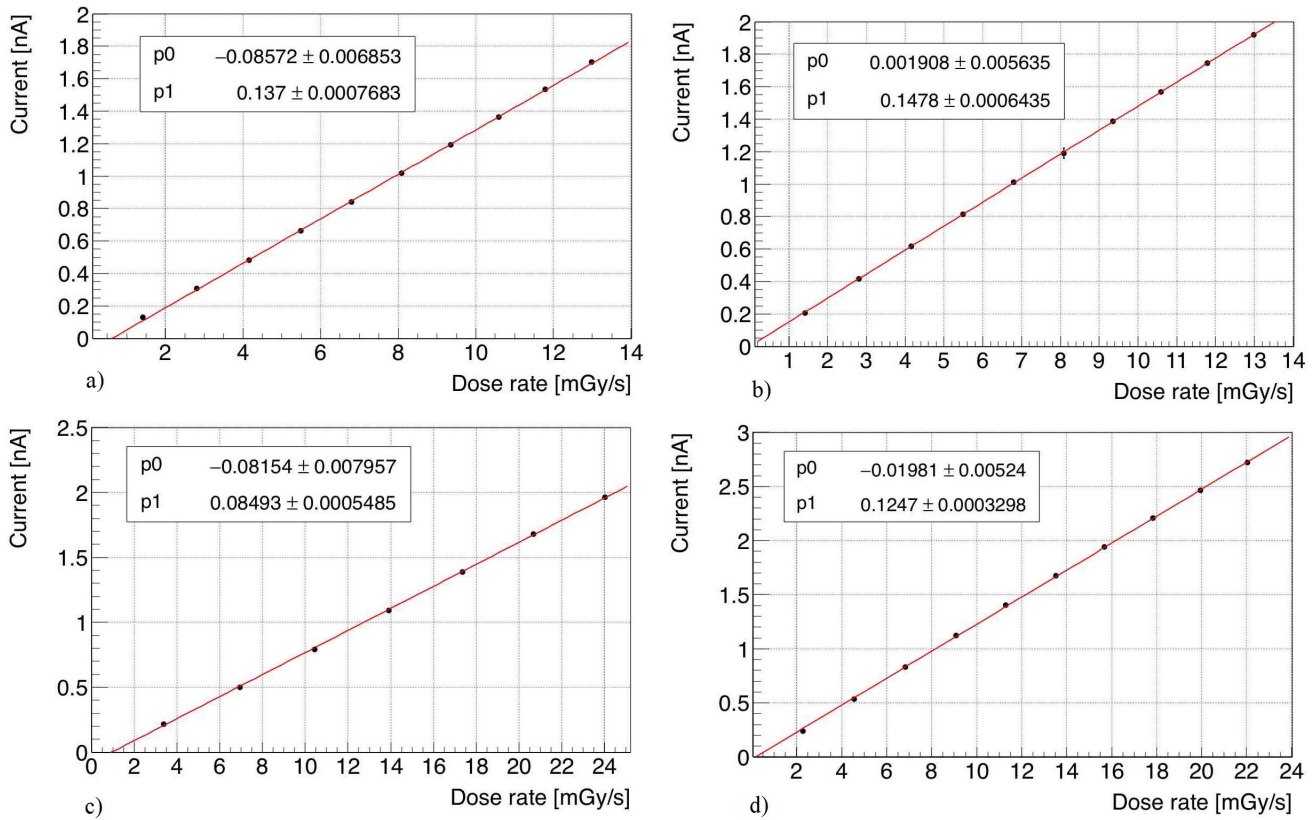


Fig.4 Current versus x-ray doses at 0V bias of various devices in a-Si:H having different layer thickness and electron selective contact materials a) AZO electron selective contacts with a-Si:H layer having 8.2 μm thickness (Sample 1) b) AZO electron selective contacts with a-Si:H layer having 8.2 μm thickness (Sample 2) c) AZO electron selective contacts with a-Si:H layer having 6.2 μm thickness d) Titanium Oxide electron selective contacts with a-Si:H layer having 8.2 μm thickness.

In figure 4 the results of the set of measurements at 0 V bias are shown, Table 2 displays the device sensitivities as calculated from the gradient of the dose linearity measurements presented in Figure 4. Also given in Table 2 is the regression coefficient of the linear fit of data in figure 4 from which we can infer an excellent linearity of the device responses with delivered dose.

Description of sample	Sensitivity (nC/cGy)	Regression coefficient of the fit
8.2 μm AZO electron selective contact. Sample 1	1.37	0.999880
8.2 μm AZO electron selective contact. Sample 2	1.48	0.999975
6.2 μm AZO electron selective contact.	0.84	0.999897
8.2 μm TiO ₂ electron selective contact.	1.25	0.999918

Table 2. Sensitivity and linear regression coefficient of the various devices at 0V bias.

Table 2 demonstrates the measured sensitivities are quite similar on the various 8.2 μm devices, and significantly lower for the 6.2 μm device as expected due to its reduced active layer thickness restricting the number of charges generated by the normally incident high energy photons. Figure 5 shows the results of the measurement of devices at 30 V bias (20 V for the 6.2 μm device).

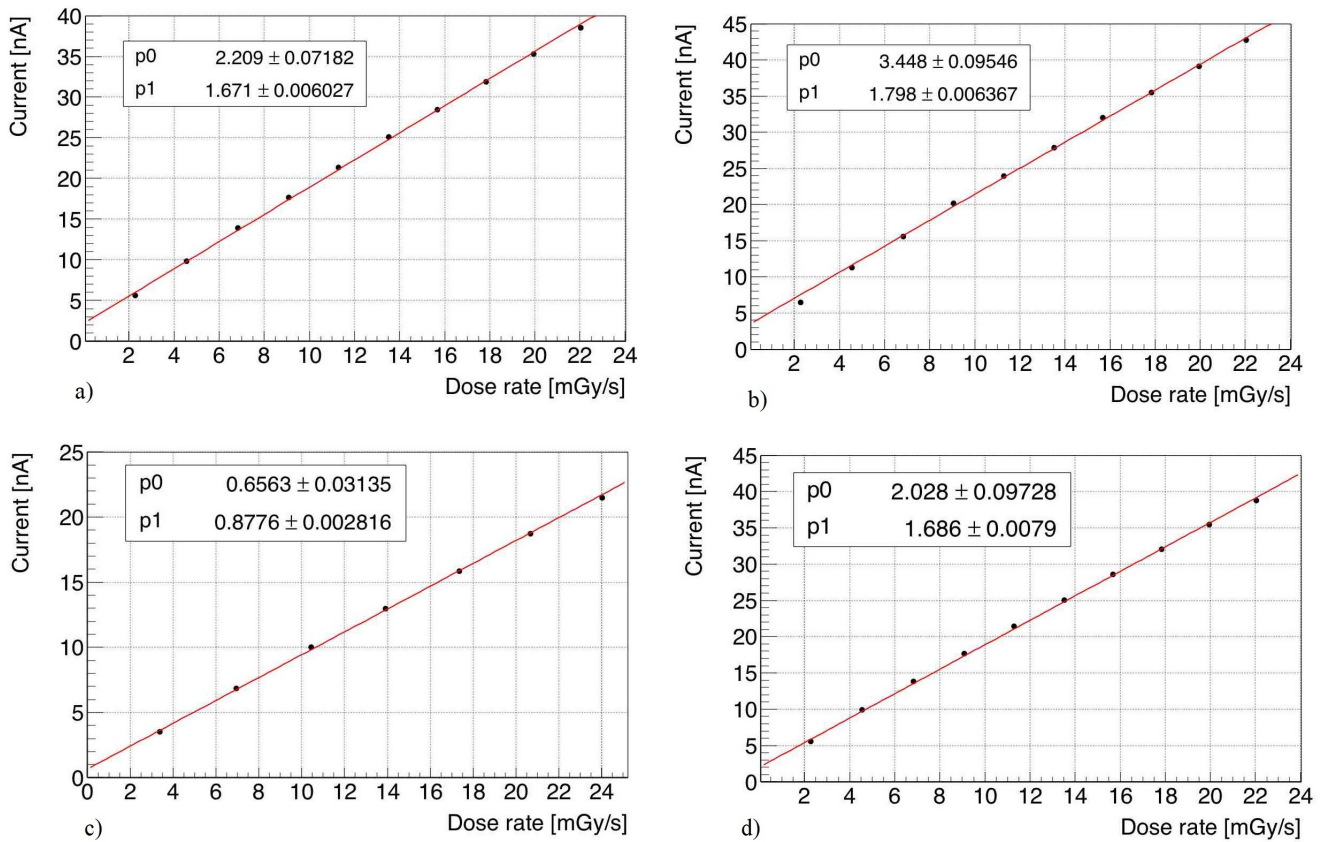


Fig.5 Current versus x-ray doses under 30 V bias of various devices in a-Si:H having different layer thickness and electron selective contact materials a) AZO electron selective contacts with a-Si:H layer having 8.2 μm thickness (Sample 1) b) AZO electron selective contacts with a-Si:H layer having 8.2 μm thickness (Sample 2) c) AZO electron selective contacts with a-Si:H layer having 6.2 μm thickness (biased at 20V) d) Titanium Oxide electron selective contacts with a-Si:H layer having 8.2 μm thickness.

Table 3 shows the calculated device sensitivities and the regression coefficient of the linear fitting applied to the results in Fig 5. Analogously with, the detector responses under a zero applied bias, we can again infer an excellent linearity of the response versus dose of the detectors when operated at an applied bias. Furthermore, the observed sensitivities for all the biased devices (30 V for 8.2 μm thick samples and 20 V for the 6.2 μm sample) show an increase by more than a factor 10 in comparison to device sensitivities at 0 V bias. While the linearities under non-zero bias are still excellent, it is worth noting the regression coefficients have slightly smaller values in devices under bias compared to device responses at 0 V bias as presented in Table 2.

Description of sample	Sensitivity (nC/cGy)	Regression coefficient of the fit
8.2 μm AZO electron selective contact. Sample 1	16.71	0.999655
8.2 μm AZO electron selective contact. Sample 2	17.98	0.999491
6.2 μm AZO electron selective contact.	8.78	0.999828
8.2 μm TiO ₂ electron selective contact.	16.86	0.999757

Table 3. Sensitivity and linear regression coefficient of the various devices under bias

4. Current versus voltage under x-ray irradiation.

Current versus voltage behavior of sample detectors under irradiation was also studied to further characterize them, with the X-ray tube configured as illustrated in figure 3 and held at fixed tube current and voltage (100 μ A and 30 kV), producing a nominal dose rate of 6.8 mGy/s. The measured data (Fig.6) shows an exponential dependence of current from bias voltage according to the fit formula:

$$I = p_0 * (1 - p_1 * e^{-p_2 * V})$$

where I is the photocurrent, V is the bias voltage and p_0 , p_1 and p_2 are fitting parameters. Extrapolating the trend and assuming no breakdown at voltages above 40 V, the fit shows a saturating behavior of the current at a bias voltage in the order of $\approx 3/p_2$ (95% of saturation current) and a saturation photocurrent in the order of p_0 . Hence, fitting the experimental data with the formula presented will allow for the determination of the saturation voltage and current of the devices. Table 4 shows the value of the saturation voltage and currents for all detectors. With the exception of the 8.2 μ m AZO electron selective contact (Sample 2) which displays exceptionally high saturation values, the other 8.2 μ m samples have similar values both in saturation current and voltage. The thinner 6.2 μ m AZO sample has lower saturation voltage and current values as expected, with the reduction factor in saturation values in the 6.2 μ m AZO sample (sample 4) in comparison to sample 1 (8.2 μ m thick device with AZO electron selective contact) closely approximating the reduction factor in the active layer thickness between these two samples.

Description of samples	Saturation Voltage [V]	Saturation Current [nA]
8.2 μ m AZO electron selective contact. Sample 1	209.2	38.48
8.2 μ m AZO electron selective contact. Sample 2	333.4	64.44
6.2 μ m AZO electron selective contact.	144.2	22.74
8.2 μ m TiO ₂ electron selective contact.	199.7	37.33

Table 4. Saturation voltages and saturation currents.

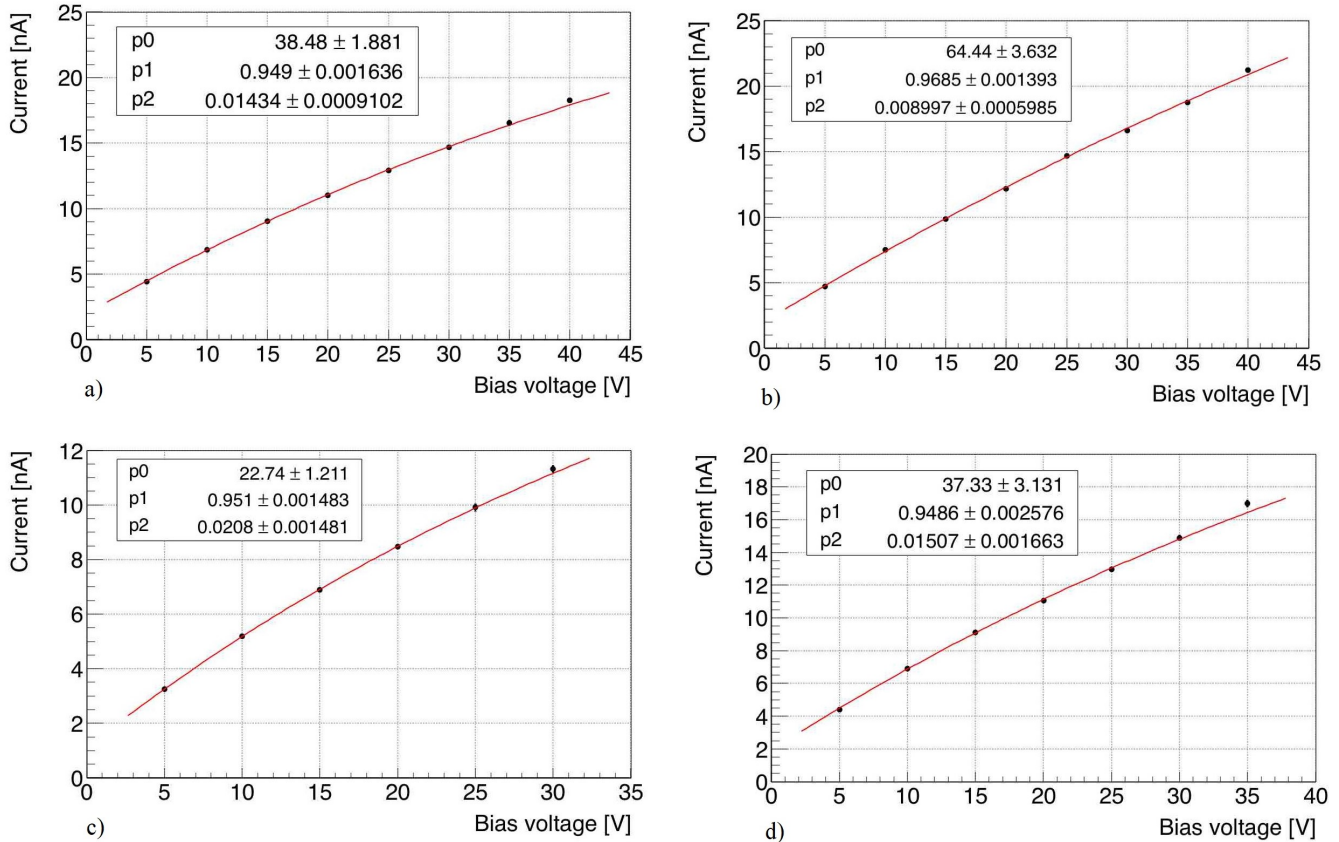


Fig.6 Current versus Bias Voltage a) fixed x-ray tube settings (100 μ A and 30 kV dose rate 6.8 mGy/s) of various devices in a-Si:H having different layer thickness and electron selective contact materials a) AZO electron selective contacts with a-Si:H layer having 8.2 μ m thickness (Sample 1) b) AZO electron selective contacts with a-Si:H layer having 8.2 μ m thickness (Sample 2) c) AZO electron selective contacts with a-Si:H layer having 6.2 μ m thickness (biased at 20V) d) Titanium Oxide electron selective contacts with a-Si:H layer having 8.2 μ m thickness.

5. Conclusions.

This work presents investigations into the use of charge carrier selective contacts for the fabrication of hydrogenated amorphous silicon diodes for x-ray detection applications using a 3D structure. Two types of electron selective contacts have been tested: Titanium (TiO_2) and Aluminum doped zinc oxide (AZO). In order to assess their usability for x-ray detection, leakage current density, linearity and sensitivity have been assessed for two different thicknesses of the a-Si:H substrate. The AZO proved to be the best candidate for all a-Si:H substrate thicknesses, showing a systematic lower leakage current density between 9.2 and 14 nA/cm^2 in respect to the TiO_2 samples (over 24 nA/cm^2). The samples fabricated with the AZO contacts showed also a higher saturation voltage and current under illumination with 30 kVp x-rays. This result is confirmed also by the excellent linearity and sensitivity of the AZO samples, which peaked at a remarkable 18 nC/cGy . Thickness of the aSi:H substrate is also another important parameter to consider in the optimization of the sensitivity of the diodes: a variation of the thickness from 6.2 to 8.2 μm has generated an increment of sensitivity of more than 40% in the samples analysed in this work. In conclusion, the Aluminum Zinc Oxide has shown to be the most promising combination for the fabrication of the 3D a-Si:H diodes.

Acknowledgements

The research was funded by INFN Scientific committee 5 under the experiment name 3D-SiAm and by INFN committee for technological transfer under the experiment name INTEF-3D-SiAm. Additional funds came from Fondazione Cassa di Risparmio di Perugia (RISAI project n. 2019.0245). This work was also supported by the Australian Government Research Training Program, Australia, and the Australian Institute of Nuclear Science and Engineering Post-Graduate Research award, Australia (ALNSTU12583).

References

- [1] M. Menichelli et al. “Hydrogenated amorphous silicon detectors for particle detection, beam flux monitoring and dosimetry in high-dose radiation environment.” *JINST* **15** C04005 (2020).
- [2] U. Würfel et al. “Charge Carrier Separation in Solar Cells”, *IEEE J. of Photovoltaics* 1 (2015) 46.
- [3] Wyrsh, N.; Ballif, C. Review of amorphous silicon based particle detectors: The quest for single particle detection. *Semicond. Sci. Technol.* **2016**, *31*, 103005
- [4] <http://www.newtonscientificinc.com/50kv-10w-monoblock/>